JOURNAL OF VIROLOGY, June 1999, p. 5056–5063 Vol. 73, No. 6
0022-538X/99/$04.00+0

Dynamics of Nontypical Apoptotic Morphological Changes Visualized by Green Fluorescent Protein in Living Cells with Infectious Pancreatic Necrosis Virus Infection

JIANN-RUEY HONG,[1,2] TAI-LANG LIN,[1] JER-YEN YANG,[3] YA-LI HSU,[1]* AND JEN-LEIH WU[1]*

Laboratory of Marine Molecular Biology and Biotechnology, Institute of Zoology, Academia Sinica, Nankang, Taipei 115,[1] Graduate Institute of Life Sciences, National Defense Medical Center, Taipei 117,[2] and Institute of Marine Biotechnology, National Taiwan Ocean University, Keelung,[3] Taiwan, Republic of China

Received 12 October 1998/Accepted 26 February 1999

Morphologically, apoptotic cells are characterized by highly condensed membrane blebbing and formation of apoptotic bodies. Recently, we reported that apoptosis precedes necrosis in a fish cell line infected with infectious pancreatic necrosis virus (IPNV). In the present study, we tested the possibility that nontypical apoptosis is a component of IPNV-induced fish cell death. A variant type of green fluorescent protein (EGFP) was expressed in a fish cell line such that EGFP served as a protein marker for visualizing dynamic apoptotic cell morphological changes and for tracing membrane integrity changes during IPNV infection. Direct morphological changes were visualized by fluorescence microscopy by EGFP in living cells infected with IPNV. The nontypical apoptotic morphological change stage occurred during the pre-late stage (6 to 7 h postinfection). Nontypical apoptotic features, including highly condensed membrane blebbing, occurred during the middle apoptotic stage. At the pre-late apoptotic stage, membrane vesicles quickly formed, blebbed, and were finally pinched off from the cell membrane. At the same time, at this pre-late apoptotic stage, apoptotic cells formed unique small holes in their membranes that ranged from 0.39 to 0.78 μm according to examination by scanning electron microscopy and immunoelectron microscopy. Quantitation of the intra- and extracellular release of EGFP by CHSE-214-EGFP cells after IPNV infection was done by Western blotting and fluorometry. Membrane integrity was quickly lost during the late apoptotic stage (after 8 h postinfection), and morphological change and membrane integrity loss could be prevented and blocked by treatment with apoptosis inhibitors such as cycloheximide, genistein, and EDTA before IPNV infection. Together, these findings show the apoptotic features at the onset of pathology in host cells (early and middle apoptotic stages), followed secondarily by nontypical apoptosis (pre-late apoptotic stage) and then by postapoptotic necrosis (late apoptotic stage), of a fish cell line. Our results demonstrate that nontypical apoptosis is a component of IPNV-induced fish cell death.

Infectious pancreatic necrosis virus (IPNV) is the prototype virus of the family *Birnaviridae* (8). Birnaviruses also include infectious bursal disease virus of domestic fowl (28) and drosophila X virus of *Drosophila melanogaster* (43). IPNV causes a lethal disease in both hatchery-reared juvenile salmonids (11, 48) and nonsalmonid fish (5, 11).

There are two major morphologically and biochemically distinct modes of death in eukaryotic cells: necrosis and apoptosis (9, 18, 51). Necrosis is considered to be a pathological reaction that occurs in response to perturbations in the cellular environment, such as complement attack, severe hypoxia, and hyperthermia. These stimuli increase the permeability of the plasma membrane, resulting in irreversible swelling of the cells (51). On the other hand, apoptosis is characterized morphologically by cell shrinkage and hyperchromatic nuclear fragments and biochemically by chromatin cleavage into nucleosomal oligomers (51). Apoptosis is considered to be a physiological process involved in normal tissue turnover which occurs during embryogenesis, aging, and tumor regression (51). However, pathological stimuli, such as viral infection (14–16, 27, 29, 30), can also trigger the apoptotic process.

The integrity of the plasma membrane plays an important role in maintaining Ca^{2+} homeostasis in cells (22, 33). An essential role for the lymphocyte plasma membrane in the development of apoptosis has been proposed (1, 19, 42). It was reported that protein kinase C is activated during apoptosis induced by gamma irradiation (32) and glucocorticoids (31). This activation of protein kinase C may be related to increases in diacylglycerol, one of the earliest signal-induced breakdown products of membrane-bound inositol phospholipid.

Green fluorescent protein (GFP) from the jellyfish *Aequorea victoria* is a revolutionary report molecule for monitoring gene expression and fusion protein localization in vivo or in situ and in real time (3, 24, 33, 35, 46). In the present study, we tested whether nontypical apoptosis is a component of IPNV-induced fish cell death. A variant type of GFP (EGFP) served as a marker for the visualization of dynamic apoptotic cell morphological changes and for tracing membrane integrity changes during IPNV infection. CHSE-214 cells containing the gene for EGFP (CHSE-214-EGFP cells) were visualized by fluorescence microscopy to detect sequential morphological changes during infection with IPNV. Nontypical apoptotic morphological change occurred in the pre-late stage (6 to 7 h postinfection [p.i.]). At the pre-late stage, apoptotic cells formed unique, small holes in their membranes according to examination by scanning electron microscopy and immunoelectron microscopy. Quantitation of the intra- and extracellular release of EGFP by CHSE-214-EGFP cells after IPNV infection was examined by Western blotting and fluorometry. The morphological changes and integrity of membrane loss could be pre-

* Corresponding author. Mailing address: Laboratory of Marine Molecular Biology and Biotechnology, Institute of Zoology, Academia Sinica, Nankang, Taipei 115, Taiwan, Republic of China. Phone: 886-2-27899500. Fax: 886-2-27858059. E-mail: ZOJLWU@ccvax.sinica.edu.tw.

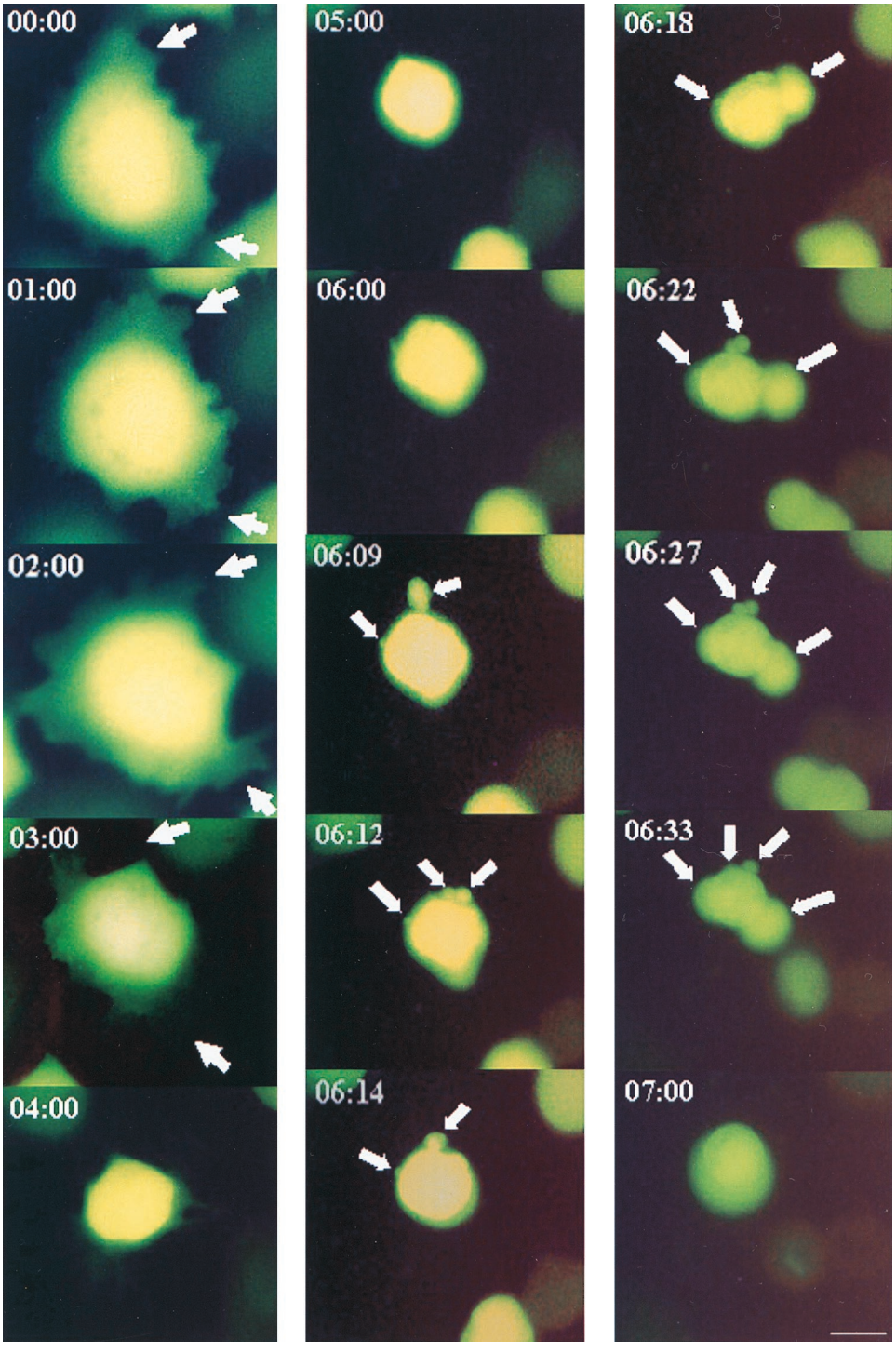

FIG. 1. Dynamics of the sequential morphological changes visualized by EGFP in living cells infected with IPNV. Monolayer cultures of CHSE-214 cells were transfected with pEGFP-N1 by using Lipofectin and selected with G418. Cells were infected with virus (MOI of 1), and virus-infected cells were sequentially observed by fluorescence microscopy from 0 to 7 h p.i. Photographs were taken with a 40× objective. Scale bar, 3 μm. The arrows indicate the formation of MV from the apoptotic cell.

vented or blocked by treatment with drugs such as cycloheximide (CHX), genistein, and EDTA. Together, these findings demonstrate that nontypical apoptosis is a component of IPNV-induced apoptotic cell death in fish. In addition, these findings regarding typical to nontypical apoptotic morphological changes should provide important insights into the apoptotic process of virus infection.

MATERIALS AND METHODS

Wild-type CHSE-214 cells, CHSE-214-EGFP cells, and viruses. Chinook salmon embryo (CHSE-214) cells were obtained from the American Type Culture Collection. Cells were grown at 18°C as monolayers in plastic tissue culture flasks (Nunc) using Eagle minimum essential medium (MEM) supplemented with 10% (vol/vol) fetal calf serum (FCS) and 25 μ g of gentamicin per ml. GFP-producing cells were obtained by transfection of CHSE-214 cells with a pEGFP-N1 vector (6) and selection with G418. In these vectors, transcription of

insert sequences is driven by the immediate-early promoter of human cytomegalovirus. The coding region contains the EGFP gene, which contains a chromophore mutation which produces fluorescence 35 times more intense than that of wild-type GFP (6).

The virus isolated, E1-S, a member of the Ab strain of IPNV, was obtained from Japanese eel in Taiwan (50). E1-S was propagated in CHSE-214 cell monolayers at a multiplicity of infection (MOI) of 0.01 particles per cell. Infected cultures were incubated at 18°C until an extensive cytopathic effect was observed. The cells were scraped into a tube with the tissue culture medium and chilled on ice, and the cells were then sonicated. This virus stock (5×10^7 to 1×10^8 PFU/ml) was dispensed into 1-ml samples and stored at −70°C. Virus plaque assays were performed on confluent monolayers of CHSE-214 cells that were infected with the virus solution for 1 h at room temperature, overlaid with 0.6% agarose containing 2.5 μg of trypsin per ml, and incubated for 3 days at 18°C. Cells were then stained with 1% crystal violet in 20% ethanol (8).

Immunoblotting. About 10^5 cells per ml were seeded on a 60-mm-diameter petri dish and allowed to grow for more than 20 h. The cell monolayers were rinsed twice with phosphate-buffered saline (PBS), after which they were infected at an MOI of 1 and incubated for 0, 2, 4, 6, 8, 10, 12, and 24 h p.i. Uninfected control cells were also incubated for the same periods of time. At the end of each incubation time, the culture medium was aspirated. The cells were washed with PBS and then lysed in 0.3 ml of lysis buffer (10 mM Tris base, 20% glycerol, 10 mM sodium dodecyl sulfate [SDS], 2% β-mercaptoethanol, pH 6.8).

Proteins were separated by SDS-polyacrylamide gel electrophoresis (21), electroblotted, and subjected to immunodetection as described by Kain et al. (17). Blots were incubated with a 1:7,500 dilution of an immunoglobulin fraction (Clontech) and a 1:1,500 dilution of a peroxidase-labeled goat anti-rabbit conjugate (Amersham). Chemiluminescence detection was performed in accordance with the instructions provided with the Western Exposure Chemiluminescent Detection System (Amersham). Chemiluminescent signals were imaged by exposure of Kodak XAR-5 film (Eastman Kodak, Rochester, N.Y.). Stripping and reprobing of the Western blot (17) and removal of the primary and secondary antibodies from blot were achieved by incubation in stripping buffer containing 62.5 mM Tris-HCl (pH 6.8), 3.0% (wt/vol) SDS, and 50 mM 1,4-dithiothreitol for 30 min at 55°C with gentle shaking. The blot was washed three times in PBS containing 0.1% (vol/vol) Tween 20 for 10 min each time and reprobed with antibodies beginning at the membrane blocking step.

Experiments examining the potency of drugs for preventing morphological change and blocking membrane integrity loss and those examining subsequent EGFP retention during virus infection and incubation were carried out as described above, except that extra CHX (10 μg/ml), aprotinin (400 μg/ml), leupeptin (400 μg/ml), genistein (100 μg/ml), tyrphostin (100 μg/ml), and EDTA (2 mM) were added to CHSE-214 cells before virus infection and incubation for 16 h. At the end of the incubation period, cells were harvested and samples were analyzed by Western blotting as previously described (17).

Fluorescence microscopy. A CHSE-214-EGFP monolayer infected with IPNV (MOI = 1) was examined by light and fluorescence microscopy using an Olympus IX70 microscope equipped with a BP450-480 pass excitation filter and a BA515 barrier emission filter for observation of EGFP fluorescence. Photographs were taken with a C-35 AD-4 camera using Kodak Ektachrome 200 film.

DNA preparation and gel electrophoresis. About 10^5 cells per ml were seeded on a 60-mm-diameter petri dish and allowed to grow for more than 20 h. The cell monolayers received virus at an MOI of 1.0 and were incubated for 8 h. Uninfected control cells were also incubated for 8 h. The two groups were used for DNA fragmentation studies. At the end of incubation, the cells were lysed with lysis buffer (10 mM Tris-HCl, 0.25% Triton X-100, 1 mM EDTA, pH 7.4). After treatment with phenol-chloroform-isoamyl alcohol (25:24:1), the DNA was precipitated in the presence of 0.3 M sodium acetate and cold absolute ethanol at −70°C for 2 h and then resuspended in 10 mM Tris-HCl (pH 7.4)–1 mM EDTA. Aliquots of 20 μl containing approximately 5 to 10 μg of DNA were then electrophoresed in 1.2% agarose gels for 2 h at 40 V. Gels were stained with ethidium bromide and photographed under UV transillumination.

Scanning electron microscopy. Scanning electron microscopy analysis was carried out by cell seeding on a two-chamber slide. CHSE-214 cells were infected with virus at an MOI of 1 and incubated for 0, 4, 8, and 12 h. At the end point, cells were washed twice with PBS and fixed with 2.5% glutaraldehyde in 0.1 M phosphate buffer. Samples were postfixed with OsO_4, dehydrated in ethanol, critical point dried, and gold sputtered. A Philips 515 scanning electron microscope was used to examine the specimens.

Immunoelectron microscopy. CHSE-214-EGFP cells were infected at an MOI of 1. Infected and uninfected control cells were harvested 8 h after infection. Thin-section electron microscopy and immunogold labeling were carried out as described by McNulty et al. (27). The grids were stained with a 1:1,000 dilution of GFP-specific polyclonal antiserum and a 1:50 dilution of a 15-nm gold-labeled goat anti-rabbit immunoglobulin G conjugate.

Quantitation of EGFP release by CHSE-214-EGFP cells. Cellular EGFP and culture medium EGFP protein samples were prepared for assay in EGFP release experiments. About 10^5 cells per ml were seeded on a 60-mm petri dish for more than 20 h. Cell monolayers were rinsed twice with PBS and then cultured in 3 ml of 10% FCS-containing MEM. Uninfected cells used as a normal control and cells that received virus at an MOI of 1 were incubated for 0, 2, 4, 6, 8, 10, 12, and 24 h p.i. At the end of each incubation period, the culture medium was collected to determine the concentration of retained EGFP. Cells were washed with PBS and then lysed in 0.3 ml of lysis buffer (10 mM Tris base, 20% glycerol, 10 mM SDS, 2% β-mercaptoethanol, pH 6.8).

The assay procedure was as follows. First, recombinant GFP purchased from Clontech was used as the standard. The GFP standard was diluted from 1 μg/0.1 ml to 0.001 μg/0.1 ml with 10% FCS-containing MEM. Second, 5 μg of lysed cells per sample was diluted with 10% FCS-containing MEM to a final volume of 100 μl. Third, the supernatant was assayed, and 30 μg of supernatant per sample was diluted with 10% FCS-containing MEM to a final volume of 100 μl. Protein concentration was determined by the dye-binding method of Bradford (2) using a commercially available kit (Bio-Rad, Richmond, Calif.) with bovine serum as the standard. Fourth, the fluorescence intensity of three group samples was counted by a Fluorolite 1000 (DYNEX). The EGFP concentrations of the lysed cells and supernatant were evaluated by comparing them with that of the GFP standard by using a Fluorolite 1000 and dividing by 35 (6).

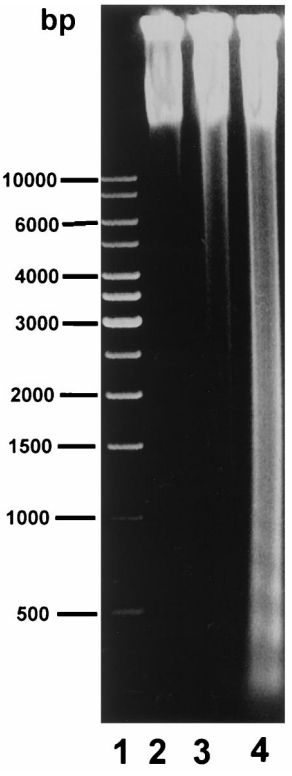

FIG. 2. DNA fragment analysis of CHSE-214-EGFP cells infected with IPNV E1-S (MOI of 1). DNA was isolated (as described in Materials and Methods) from uninfected CHSE-214 cells as a negative control after 0 (lane 2) and 8 (lane 3) h of incubation and from cells infected for 8 h with an MOI of 1 of E1-S (lane 4), electrophoresed through 1.2% agarose gels, and visualized by ethidium bromide staining. Lane 1 contained molecular size markers (1-kb DNA ladder from USA MBI Fermentas Inc. for sizing of linear fragments ranging from 500 bp to 1 kb).

RESULTS

Visualization of dynamic morphological changes by EGFP. One of the most useful aspects of GFP for biological studies is that it can be monitored in living cells (37). Figure 1 shows the sequence of morphological changes that occurred in CHSE-214-EGFP cells during virus infection (MOI = 1). These events were divided into three stages. First (early stage), detachment of the CHSE-214-EGFP cell matrix was initiated between 0 and 3 h p.i. Second (middle stage), the whole cell was rounded up and appeared morphologically more compact. In this period (3 to 6 h p.i.), the cell volume decreased to one-third of its original size and the fluorescence intensity was enhanced. In the third (pre-late) stage, the cells at 6 to 7 h p.i. quickly underwent severe morphological changes. Membrane vesicles (MV) were formed from the plasma membrane, and

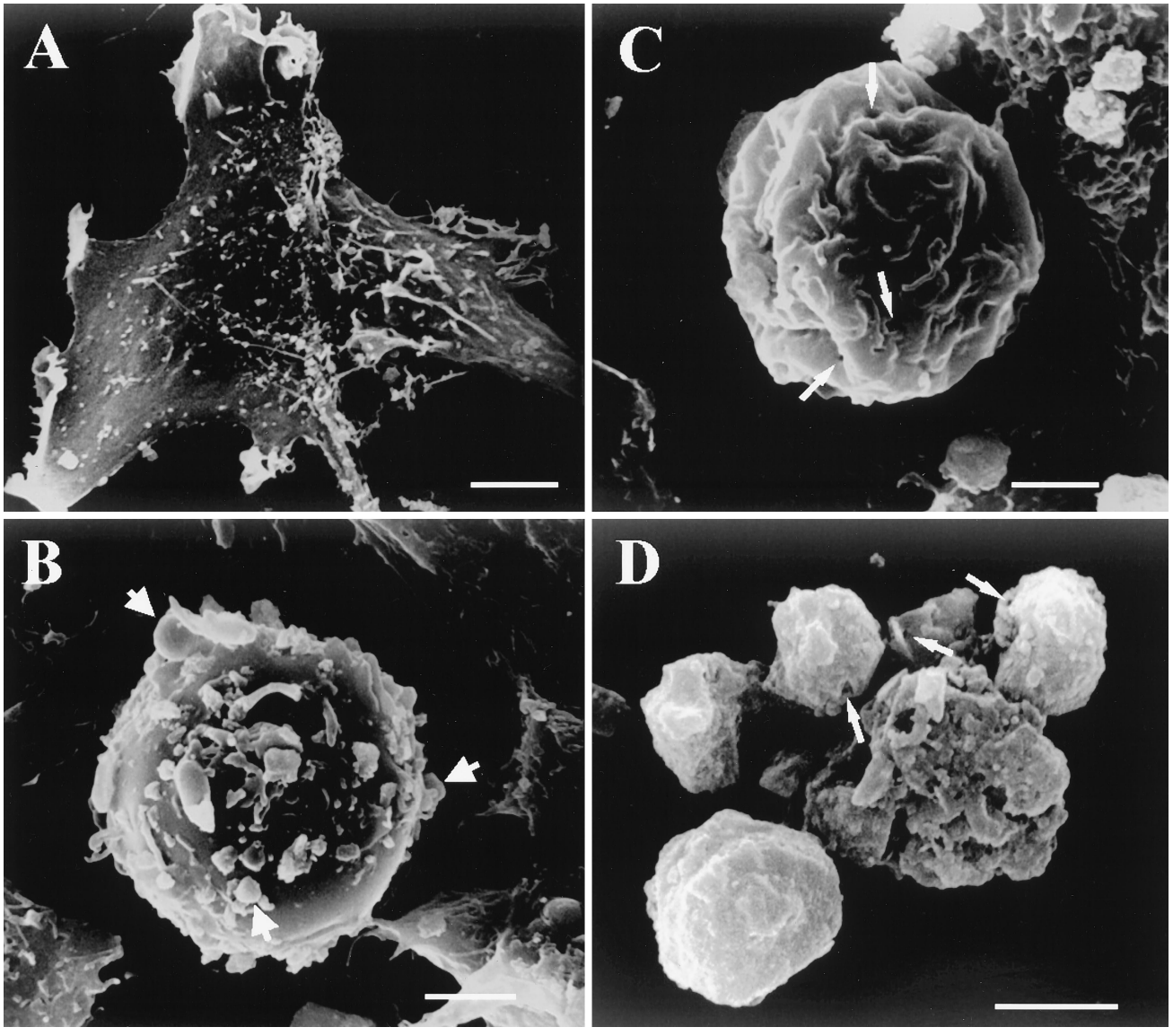

FIG. 3. Scanning electron micrographs of CHSE-214 cells. (A) Negative control CHSE-214 cell. (B) Pre-late apoptotic CHSE-214 cell. The formation of MV from the apoptotic cell is indicated by arrows. (C) Middle-late apoptotic cell. The formation of small holes is indicated by arrows. (D) Late apoptotic cell. Small holes left on the surfaces of apoptotic bodies from the IPNV-treated group are indicated by arrows. Scale bar, 1.5 μm.

these vesicles eventually blebbed and finally pinched off from the cell membrane.

Induction of internucleosomal cleavage by IPNV in CHSE-214-EGFP cells. We examined the effect of IPNV infection on host DNA in CHSE-214-EGFP cells since DNA fragmentation is a well-defined biochemical marker of apoptosis (40). Virus (MOI = 1)-infected cells were examined for evidence of internucleosomal fragmentation. Intense internucleosomal fragmentation of DNA, a pattern highly specific to apoptosis, was observed in CHSE-214-EGFP cells infected with IPNV (Fig. 2). The IPNV induced DNA fragmentation at 8 h p.i. (Fig. 2, lane 4). The negative control showed no DNA fragmentation at 0 and 8 h of incubation (Fig. 3, lanes 2 and 3). Lane 1 contained molecular weight markers that ranged from 500 bp to 1 kb (from MBI Fermantas Inc.).

Ultrastructural morphology changes in IPNV-infected CHSE-214 cells detected by scanning electron microscopy. Apoptosis induces characteristic morphological changes in cells, such as condensation and fragmentation of the nucleus, as well as loss of cytoplasm (54). To substantiate further that IPNV-infected cells had undergone nontypical apoptotic morphological changes such that membrane integrity changed, negative control and IPNV-infected CHSE-214 cells were harvested and processed for scanning electron microscopy as shown in Fig. 3. Negative control cells are shown in Fig. 3A. IPNV-infected CHSE-214 cells at 8 h p.i. displayed detachment, cell rounding, and blebbing of MV from the plasma membrane at the pre-late stage of apoptosis (20%; $P < 0.05$), as shown in Fig. 3B. Middle-late-stage apoptotic cells (23%; $P < 0.05$) are shown in Fig. 3C. The cell membrane appears shrunken, and holes are present in the plasma membrane. The hole sizes ranged from 0.39 to 0.78 μ m with about 10 to 20 holes per cell. A late-stage apoptotic cell (2%; $P < 0.05$) is shown in Fig. 3D with the small holes still on the surface of the late-apoptotic cell.

EGFP release is prevented by a protein synthesis inhibitor and a tyrosine kinase inhibitor. In EGFP release experiments, EGFP was used to monitor the integrity of the plasma membrane during apoptosis. As described above, small holes appeared in middle-late-stage apoptotic cells (Fig. 3C). We previously proposed that intracellular material might leak out of these small holes to the extracellular region before secondary necrosis (13). The use of EGFP to monitor the integrity of the plasma membrane of IPNV-infected CHSE-214-EGFP cells is shown in Fig. 4. The EGFP release Western blot assay result is shown in Fig. 4A. Fig. 4A, part a, shows that the amount of GFP decreased, especially between 8 and 16 h p.i. The internal control, actin protein, is shown in Fig. 4A, part b. Detection of the EGFP released from the intracellular to the extracellular region during IPNV infection is shown in Fig. 4A, part c. The increase of GFP release began between 8 and 16 h p.i., which is consistent with Fig. 4A, part a. These data indicate that the membrane integrity changed quickly at the middle-late apoptotic stage. The fluorometric EGFP release assay results are shown in Fig. 4B. The open squares show that the intracellular amount of EGFP sharply decreased from 6 to 24 h p.i. but that the largest release of EGFP occurred between 12 and 24 h p.i. The open diamonds show that the extracellular amount of EGFP increased between 6 and 24 h p.i., which matches the intracellular data described above.

EGFP was also used as a protein indicator to directly probe membrane integrity by immunoelectron microscopy. Normal CHSE-214-EGFP cells used as controls are shown in Fig. 5A. Figure 5B shows that the small vesicle escaped from the membrane hole at the pre-late apoptotic cell stage and that the vesicle contains the same EGFP labeled by an anti-GFP polyclonal antibody-gold complex.

Drugs, including the protein synthesis inhibitor CHX, the serine proteinase inhibitors aprotinin and leupeptin, the tyrosine kinase inhibitors genistein and tyrphostin, and the cation chelator EDTA, were used before IPNV infection to test the viability of preventing membrane integrity change. Some of the drugs, such as CHX at 10 μg/ml and 2 mM EDTA, completely prevented EGFP release, and genistein at 100 μg/ml partially prevented EGFP release (as shown in Fig. 6A) to the extracellular region (as shown in Fig. 6C). The serine proteinase inhibitors aprotinin (400 μg/ml) and leupeptin (400 μg/ml) (Fig. 6C, lanes 5 and 6, respectively) and the tyrosine kinase inhibitor tyrphostin (100 μg/ml) (Fig. 6C, lane 8) did not prevent EGFP release. The internal control, actin protein, is shown in Fig. 6B for quantitation of protein loading per sample.

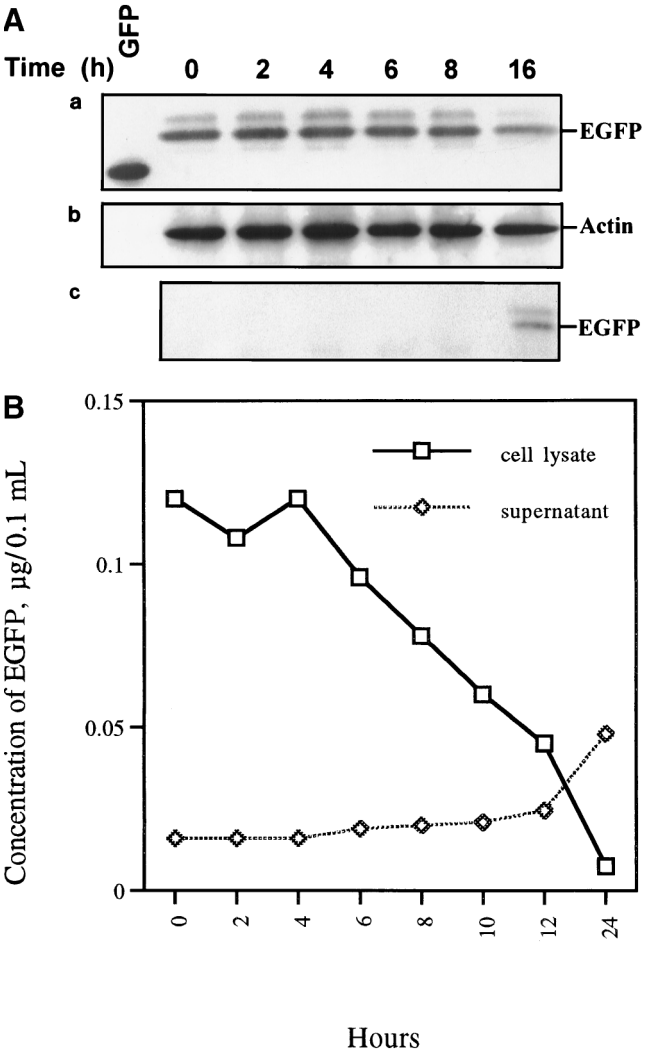

FIG. 4. Patterns of EGFP release by CHSE-214-EGFP cells infected with IPNV. (A, parts a to c) Detection of EGFP release pattern due to IPNV infection by Western blotting. CHSE-214-EGFP cells were infected with IPNV (MOI of 1). Samples were electrophoresed on an SDS-polyacrylamide gel and electroblotted to a nitrocellulose membrane. The membrane either contained a rabbit polyclonal antiserum directed against EGFP (part a and c) or was stripped and reprobed with a mouse IgG monoclonal antibody directed against actin (part b). The chemiluminescent signal was imaged on Kodak XAR-5 film using a 3-min (part a), 1.5-min (part b), or 30-min (part c) exposure. (a) Lanes: 1, 0.45 μg of wild-type GFP; 2 to 7, 30 μg of virus-infected CHSE-214 cell lysate at 0, 2, 4, 6, 8, and 16 h p.i., respectively. (b) The nitrocellulose membrane in part a was stripped and reprobed with anti-actin monoclonal IgG. (c) A 30-μg sample of supernatant protein of IPNV-infected CHSE-214-EGFP cells at 0, 2, 4, 6, 8, 10, 12, and 24 h p.i., respectively. (B) Rate of EGFP release by CHSE-214-EGFP cells infected with IPNV. Cellular and culture medium EGFP samples were prepared for assay in EGFP release experiments. About 10^5 cells per ml were seeded on a 60-mm petri dish and incubated for more than 20 h. Cells that received virus at an MOI of 1 were incubated for 0, 2, 4, 6, 8, 10, 12, and 24 h p.i. At the end of each incubation time, the IPNV-infected CHSE-214 cells and culture medium were collected to determine the concentration of retained EGFP. Both 5 μg of lysed virus-infected cells per sample and 30 μg of supernatant medium per sample were counted by a Fluorolite 1000. The EGFP concentrations of the lysed cells and supernatant were evaluated by using a Fluorolite 1000 to compare them with standard GFP protein and dividing by 35 (6).

DISCUSSION

Here, we provide the first evidence that GFP can be used to sequentially monitor apoptotic morphological changes in living cells or probe the change in membrane integrity after IPNV infection. GFP is stable and species independent and can be monitored noninvasively in living cells (25, 37). A clone with strong fluorescence intensity and normal morphology, CHSE-214-EGFP, was selected and subcloned as a cell line for experiments (as shown in Fig. 1). The clones with lower fluorescence intensity did not produce a good image in sequential morphology studies (4, 10). Working with GFP raises practical problems. One such problem, common in fluorescence microscopy of live cells, is that of phototoxicity, which is thought to be caused mainly by fluorophore-mediated generation of free radicals. Fortunately, the introduction of mutant GFPs with higher quantum efficiencies, lower-energy excitation spectra, and better temperature stability (6, 12, 41) has been advantageous and has significantly widened the applicability of GFP to the study of proteins of low abundance. If the cameras and fluorescence microscopes used become more and more sensitive and efficient, the problems will be further alleviated.

In our system, cloned cells were expressed with EGFP (32.5

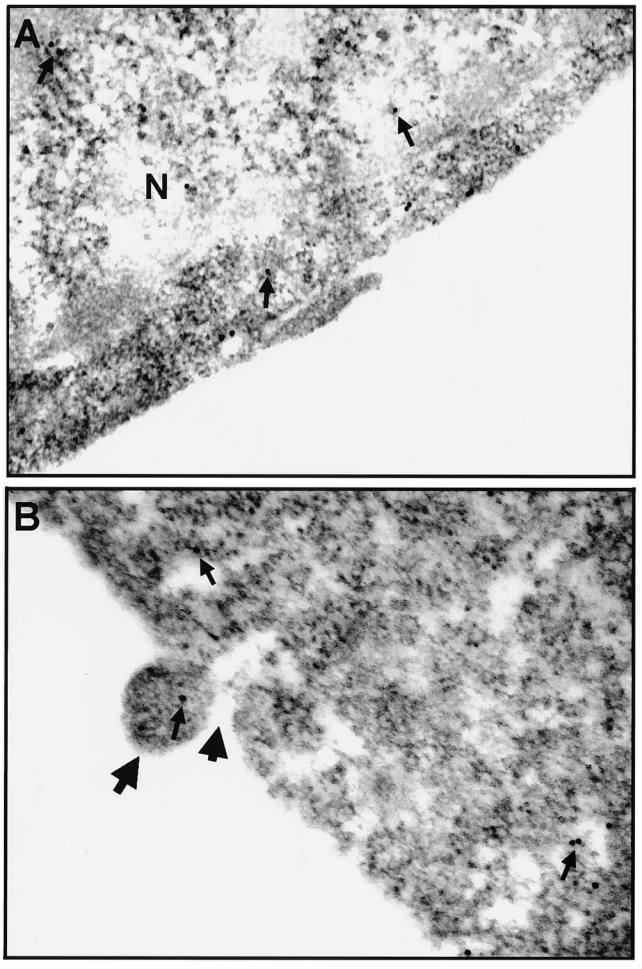

FIG. 5. Immunoelectron micrographs of ultrathin sections of CHSE-214-EGFP cells that were uninfected or infected with IPNV and labeled with anti-GFP IgG. (A) Normal CHSE-214-EGFP cell used as a negative (N) control on which labeled EGFP is present (arrows) and EGFP formed dimers. (B) CHSE-214-EGFP cell infected with IPNV (MOI of 1) at 8 h p.i. upon which labeled EGFP is present (small arrows). Nontypical apoptotic morphological changes were observed at this pre-late apoptotic cell stage such as the formation of MV (large, long arrow) and, finally, the MV pinching off from the plasma membrane of the apoptotic cell (large, short arrow).

kDa; as shown in Fig. 4A, lane 2), which is larger in molecular size than wild-type GFP (27 kDa; as shown in Fig. 4A, lane 1). EGFP may occur by glycosylation or phosphorylation in CHSE-214 cells and appears to have a larger molecular size than wild-type GFP. In addition, GFP is fluorescent either as a monomer or as a dimer. The ratio of monomeric to dimeric forms depends on the protein concentration and the environment (47). As described above, EGFP was also found in both control cells and IPNV-infected cells either as a monomer or as a dimer (as shown in Fig. 5). We found a doublet EGFP from the released EGFP, as shown in Fig. 4A (part c, lane 6) and 6C, but whether posttranslational modification of EGFP can be enhanced by dimerized EGFP could not be ascertained. To substantiate the significance of our findings, further experiments are required to evaluate how EGFP produces different expression patterns in our system.

EGFP was used to monitor the dynamic morphological changes in CHSE-214-EGFP cells infected with IPNV. The results are shown in Fig. 1. We briefly divided this series of events into four stages: (i) the early apoptotic stage (0 to 3 h p.i.), (ii) the middle apoptotic stage (3 to 6 h p.i.), (iii) the pre-late apoptotic stage (6 to 7 h p.i.), and (iv) the postapoptotic necrosis stage (after 7 h p.i.). The morphological changes in apoptotic cells observed included cell detachment, rounding up, formation of MV, pinched off MV floating away in the culture medium, and finally, postapoptotic necrosis, as previously observed by Hong et al. (13). We found that these sequential morphological change events were different from typical apoptotic morphological changes, such as detachment, rounding up, membrane blebbing, and finally the formation of apoptotic bodies, as described by Wyllie et al. (52) and Majno and Joris (23). Here, we clearly defined this process of nontypical apoptotic morphological change by probing with EGFP after IPNV infection, and we summarize these findings in Fig. 7.

To determine the loss of membrane integrity in apoptotic cells, we used the protein marker EGFP to monitor membrane integrity change after IPNV infection (as shown in Fig. 4). The direct changes in membrane integrity identified by immunoelectron microscopy are shown in Fig. 5. The harmful membrane changes can be prevented by drugs such as the protein synthesis inhibitor CHX, and the cation chelator EDTA and can be partially prevented by the tyrosine kinase inhibitor genistein (as shown in Fig. 6).

The important role of *bcl-2* in supporting cell survival has been well demonstrated, in particular by studies with *bcl-2* transgenic (26) or knockout (45) mice. Mcl-1 is a member of the Bcl-2 family that was identified by differential screening of cDNA libraries derived from a human myeloid leukemia cell line induced to undergo differentiation in culture (20). It was

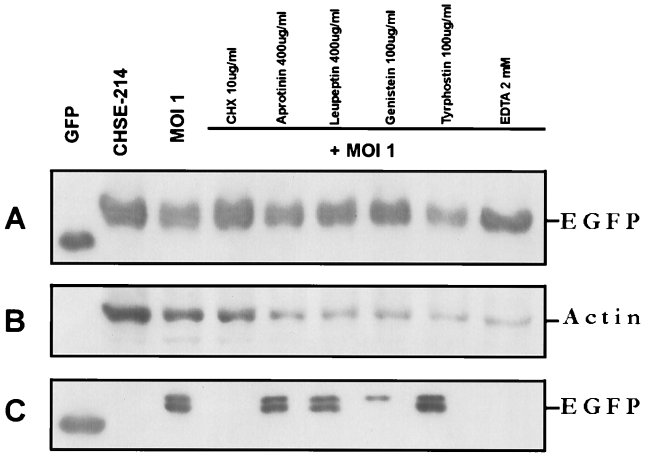

FIG. 6. Western blot assay of the effect of chemical inhibitors on EGFP release. Protein synthesis inhibitors, serine proteinase inhibitors, tyrosine kinase inhibitors, and a cation chelator were added to CHSE-214-EGFP cells before infection with IPNV (MOI of 1). After infection, the cells were incubated for 16 h. Samples were electrophoresed on an SDS–12% polyacrylamide gel and electroblotted to a nitrocellulose membrane. Antigen-specific signals were detected with either rabbit anti-GFP serum (A and C) or a mouse IgG monoclonal antibody directed against actin (B). The chemiluminescent signal was imaged on Kodak XAR-5 film by using a 5-min (A), a 1-min (B), or a 30-min (C) exposure. (A) Lanes: 1, 0.2 μg of recombinant wild-type GFP as a positive control; 2, normal CHSE-214-EGFP cell lysate; 3, 30 μg of cell lysate protein corresponding to treatment with CHX (100 μg/ml), aprotinin (400 μg/ml), leupeptin (400 μg/ml), genistein (100 μg/ml), tyrphostin (100 μg/ml), and EDTA (2 mM) and then virus infected for 16 h, respectively. (B) The nitrocellulose membrane from panel A was stripped and reprobed with an actin antibody. (C) Lanes: 1, 100 ng of wild-type GFP; 2, 30 μg of supernatant medium protein from IPNV-infected cells at 16 h p.i. 4 to 9, 30 μg of supernatant medium protein corresponding to treatment with CHX (100 μg/ml), aprotinin (400 μg/ml), leupeptin (400 μg/ml), genistein (100 μg/ml), tyrphostin (100 μg/ml), and EDTA (2 mM) before virus infection and at 16 h p.i., respectively.

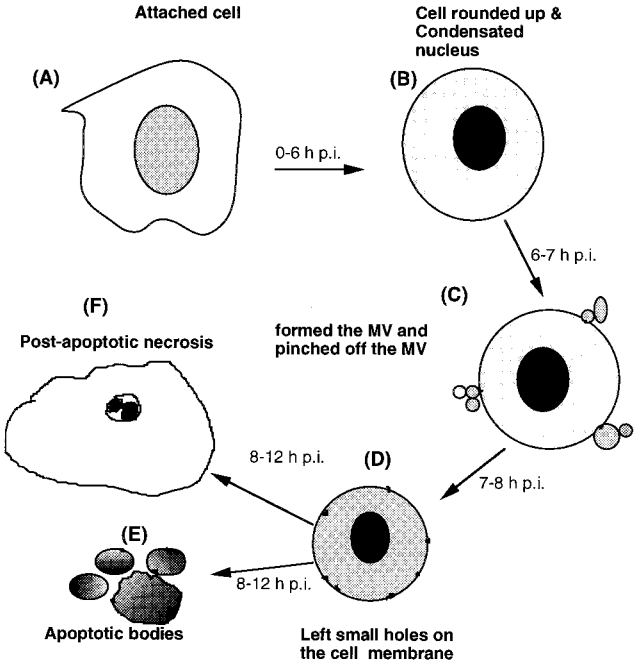

FIG. 7. Diagram illustrating the morphological changes induced in fish cells by IPNV infection. (A) Normal attached cell. In the early stage of apoptosis, the cell detaches from the extracellular martix (A to B, 0 to 3 h p.i.). In the middle stage, the apoptotic cell is rounded up (A to B, 3 to 6 h p.i.). To enter this pre-late apoptotic stage (B to C, 6 to 7 h p.i.), there is a rapid process which follows that includes MV formation and MV pinching off from the plasma membrane. In the middle stage, the apoptotic cell is left with small holes in the cell membrane (C to D, 7 to 8 h p.i.). Finally, in the late apoptotic stage, either membrane-bound apoptotic bodies (D to E, 8 to 12 h p.i.) are formed or a postapoptotic necrosis process occurs (D to F, 8 to 12 h p.i.) in which the condensed chromatin encloses the nuclear membrane.

recently shown that transfection of Mcl-1 into Chinese hamster ovary cells leads to inhibition of apoptosis induced by c-*myc* overexpression (36), implying that *mcl-1* is an inhibitor of cell death. In our system, the study of the apoptotic cell death mechanism during IPNV E1-S (MOI = 1) infection of CHSE-214-EGFP cells showed that IPNV E1-S-induced cell death may be correlated to down-regulation in the Bcl-2 family's Mcl-1 protein expression level (data not shown). We then tested whether Mcl-1 expression down-regulation can be prevented by apoptosis inhibitors such as protein synthesis inhibitors, a cation chelator, serine proteinase inhibitors, and tyrosine kinase inhibitors. When CHSE-214-EGFP cells were treated with the protein synthesis inhibitor CHX at 10 μg/ml, the cation chelator EDTA at 2 μM, and the tyrosine kinase inhibitor genistein at 100 μg/ml before IPNV infection, viral protein synthesis was blocked and Mcl-1 was partially down-regulated. However, the serine proteinase inhibitors aprotinin and leupeptin (each at 400 μg/ml) and tyrphostin at 100 μg/ml did not have the same effects (data not shown). These results are consistent with those of the EGFP release experiments described above. We suggest that the viral protein might be directly or indirectly correlated to down-regulation of the Mcl-1 expression level during apoptotic death caused by IPNV infection. However, to substantiate the significance of our findings, further experiments are required to evaluate how viral proteins relate to down-regulation of the Mcl-1 expression level.

IPNV is a highly contagious disease of susceptible hatchery-reared salmonids (11, 48) and nonsalmonid fish (13, 44). As the name indicates, infection of trout produces marked pancreatic necrosis, but histopathologic changes sometimes also occur in adipose tissue, in renal hematopoietic tissue, in the gut, and in the liver (39). We have shown that IPNV can induce nontypical apoptosis with all of its associated characteristics, including DNA fragmentation, detachment, cell rounding, membrane blebbing, formation of MV that pinch off from the cell membrane, and finally, postapoptotic necrosis from middle-stage apoptotic cells. Necrotic cell death may occur during natural infections, but these features support the hypothesis that IPNV causes CHSE-214-EGFP cells to undergo apoptosis, then nontypical apoptosis, and finally, postapoptotic necrosis in vitro.

ACKNOWLEDGMENTS

We thank R. C. Chen for reviewing the manuscript and providing comments.

This work was supported by grants awarded to Jen-Leih Wu by the National Science Council, Republic of China.

REFERENCES

1. **Ashwell, J. D., R. H. Schwartz, J. B. Mitchell, and A. Russo.** 1986. Effect of gamma radiation on resting B lymphocytes. J. Immunol. **136:**3649–3656.
2. **Bradford, M.** 1976. A rapid and sensitive method for the quantitation of microgram quantities of protein utilizing the principle of protein-dye binding. Anal. Biochem. **72:**248–251.
3. **Chalfie, M., Y. Tu, G. Euskirchen, W. W. Ward, and D. C. Prasher.** 1994. Green fluorescent protein as a marker for gene expression. Science **263:**802–805.
4. **Chen, C. S., M. Huang, S. Mrksich, G. M. Whitesides, and D. E. Ingber.** 1997. Geometric control of cell life and death. Science **276:**1425–1428.
5. **Chen, S. N., S. C. Chi, J. J. Guu, J. C. Chen, and G. H. Kou.** 1984. Pathogenicity of a birnavirus isolated from loach, Misgunus anguillicanbulayus. COA Fisheries series no. 10. Fish Dis. Res. **VI:**6–11.
6. **Cormack, B. P., R. H. Valdivia, and S. Falkow.** 1996. FACS-optimized mutants of the green fluorescent protein (GFP). Gene **173:**33–38.
7. **Dobos, P.** 1977. Virus-specific protein synthesis in cells infected by infectious pancreatic necrosis virus. J. Virol. **21:**242–258.
8. **Dobos, P., B. J. Hill, R. Hallett, D. T. C. Kells, H. Becht, and D. Tenings.** 1979. Biophysical and biochemical characterization of five animal viruses with bisegmented double-stranded RNA genomes. J. Virol. **32:**593–605.
9. **Duvall, E., and A. H. Wyllie.** 1986. Death and the cell. Immunol. Today **7:**115–119.
10. **Frisch, S. M., and E. Ruoslahti.** 1997. Integrins and anoikis. Curr. Opin. Cell Biol. **9:**701–706.
11. **Hedrick, P. P., J. L. Fryer, S. N. Chen, and G. H. Kou.** 1983. Characteristics of four birnaviruses isolated from fish in Taiwan. Fish Pathol. **18:**91–97.
12. **Heim, R., and R. Y. Tsien.** 1996. Engineering green fluorescent protein for improved brightness, longer wavelengths and fluorescence resonance energy transfer. Curr. Biol. **6:**178–182.
13. **Hong, R. H., L. L. Tai, Y. L. Hsu, and J. L. Wu.** 1998. Apoptosis precedes necrosis of fish cell line by infectious pancreatic necrosis virus. Virology **250:**76–84.
14. **Inoue, Y., M. Yasukawa, and S. Fujita.** 1997. Induction of T-cell apoptosis by human herpesvirus 6. J. Virol. **71:**3751–3759.
15. **Jacotot, E., B. Krust, C. Callebaut, A. G. Laurent-Crawford, J. Blanco, and A. G. Hovanessian.** 1997. HIV envelope glycoproteins-mediated apoptosis is regulated by CD4 dependent and independent mechanisms. Apoptosis **2:**47–60.
16. **Jeurissen, S. H. M., F. Wagenaar, J. M. A. Pol, A. J. van der Eb, and M. H. M. Noteborn.** 1992. Chicken anemia virus causes apoptosis of thymocytes after in vivo infection and of cell lines after in vitro infection. J. Virol. **66:**7383–7388.
17. **Kain, S. R., K. Mai, and P. Sinai.** 1994. Human multiple tissue Western blots: a new immunological tool for the analysis of tissue-specific protein expression. BioTechniques **17:**982–987.
18. **Kerr, J. F. R., and B. V. Harmon.** 1991. Definition and incidence of apoptosis: an historical perspective, p. 5–29. *In* L. D. Tome: and F. O. Cope (ed.), Apoptosis: the molecular basis of cell death. Cold Spring Harbor Laboratory Press, Cold Spring Harbor, N.Y.
19. **Konings, A. W. T.** 1981. Dose-rate effects on lymphocyte survival. J. Radiat. Res. **22:**282–285.
20. **Kozopas, K. M., T. Yang, H. L. Buchan, P. Zhou, and R. W. Craig.** 1993. *mcl-1*, a gene expressed in programmed myeloid differentiation, has sequence similarity to *bcl-2*. Proc. Natl. Acad. Sci. USA **90:**3516–3520.
21. **Laemmli, U. K.** 1970. Cleavage of structural proteins during the assembly of the head of bacteriophage T4. Nature **227:**680–685.
22. **Lucy, J. A.** 1972. Functional and structural aspects of biological membranes:

a suggested structural role for vitamin E in the control of membrane permeability and stability. Ann. N. Y. Acad. Sci. **203:**4–11.
23. **Majno, G., and I. Joris.** 1995. Apoptosis, oncosis, and necrosis: an overview of cell death. Am. J. Pathol. **146:**3–15.
24. **Maniak, M., R. Rauchenberger, R. Albrecht, J. Murphy, and G. Gerisch.** 1995. Coronin involved in phagocytosis: dynamics of particle-induced relocalization visualized by a green fluorescent protein tag. Cell **83:**915–924.
25. **Marshall, J.** 1995. The jellyfish green fluorescent protein: a new tool for studying ion channel expression and function. Neuron **14:**211–215.
26. **McDonnell, T. J., N. Deane, F. M. Platt, U. Jaeger, J. P. McKearn, and S. J. Korsmeyer.** 1989. *bcl-2*-immunoglobulin transgenic mice demonstrate extended B cell survival and follicular lymphoproliferation. Cell **57:**79–88.
27. **McNulty, M. S., T. J. Connor, F. McNeilly, M. F. McLoughlin, and K. S. Kirkpatrick.** 1990. Preliminary characterization of isolates of chicken anemia agent from the United Kingdom. Avian Pathol. **19:**67–73.
28. **Müller, H., C. Scholtissek, and H. Becht.** 1979. The genome of infectious bursal disease virus consists of two segments of double-stranded RNA. J. Virol. **31:**584–589.
29. **Noteborn, M. H. M., D. Todd, C. A. J. Verschueren, H. W. F. M. de Gauw, W. L. Curran, S. Veldkamp, A. J. Douglas, M. S. McNulty, A. J. van der Eb, and G. Koch.** 1994. A single chicken anemia virus protein induces apoptosis. J. Virol. **68:**346–351.
30. **Ohno, K. T., T. Nakano, Y. Matsumoto, T. Watari, R. Goitsuka, H. Nakayama, H. Tsujimoto, and A. Hasegawa.** 1993. Apoptosis induced by tumor necrosis factor in cells chronically infected with feline immunodeficiency virus. J. Virol. **67:**2427–2433.
31. **Ojedia, F., M. I. Guarda, C. Maldonado, and H. Folch.** 1990. Protein kinase-C involvement in thymocyte apoptosis induced by hydrocortisone. Cell. Immunol. **125:**535–539.
32. **Ojedia, F., M. I. Guarda, C. Maldonado, H. Folch, and H. Diehl.** 1992. Role of protein kinase C in thymocyte apoptosis induced by irradiation. Int. J. Radiat. Biol. **61:**663–667.
33. **Oparka, K. J., A. G. Roberts, S. Santa-Cruz, P. Boevink, D. A. M. Prior, and A. Smallcombe.** 1997. Using GFP to study virus invasion and spread in plant tissues. Nature **388:**401–402.
34. **Pascoe, G. A., and D. J. Reed.** 1989. Cell calcium, vitamin E, and the thiol redox system in cytotoxicity. Free Radic. Biol. Med. **6:**209–224.
35. **Prasher, D. C., V. K. Eckenrode, W. W. Ward, F. G. Prendergast, and M. J. Cormier.** 1992. Primary structure of the Aequorea victoria green-fluorescent protein. Gene **111:**229–233.
36. **Reynolds, J. E., T. Yang, L. Qian, J. D. Jenkinson, P. Zhou, A. Eastman, and R. W. Craig.** 1994. Mcl-1, a member of the Bcl-2 family, delays apoptosis induced by c-Myc overexpression in Chinese hamster ovary cells. Cancer Res. **54:**6348–6352.
37. **Rizzuto, R., M. Brini, P. Pizzo, M. Murgia, and T. Pozzan.** 1995. Chimeric green fluorescent protein as a tool for visualizing subcellular organelles in living cells. Curr. Biol. **5:**635–642.
38. **Rojiko, J. L., R. M. Fulton, L. J. Renanza, L. Williams, E. Copelan, C. M. Cheney, G. S. Reichel, J. C. Neil, L. E. Mathes, T. G. Fisher, and M. W. Coloyd.** 1992. Lymphocytotoxic strains of feline leukemia virus induce apoptosis in feline T4-thymic lymphoma cells. Lab. Investig. **66:**418–426.
39. **Sano, T.** 1971. Studies on viral disease of Japanese fishes. I. Infectious pancreatic necrosis of rainbow trout: pathogenicity of the isolants. Bull. Jpn. Soc. Sci. Fish. **37:**499–503.
40. **Schwartzman, R. A., and J. A. Cidlowski.** 1993. Apoptosis: the biochemistry and molecular biology of programmed cell death. Endocrinol. Rev. **14:**133–151.
41. **Siemering, K. R., R. Golbik, R. Sever, and J. Haseloff.** 1996. Mutations that suppress the thermosensitivity of green fluorescent protein. Curr. Biol. **6:**1653–1663.
42. **Sungurov, A. Y., and T. M. Sharlaeva.** 1988. Thymocyte membrane changes and modifications of interphase death. Int. J. Radiat. Biol. **53:**501–506.
43. **Teninges, D., A. Ohanessian, C. Richard-Molard, and D. Contamine.** 1979. Isolation and biological properties of Drosophila X virus. J. Gen. Virol. **42:**214–254.
44. **Ueno, Y., S. N. Chen, G. H. Kou, R. P. Hedrick, and J. L. Fryer.** 1984. Characterization of virus isolated from Japanese eel (*Anguilla japonica*) with nephroblastoma. Bull. Inst. Zool. Acad. Sin. **23:**47–55.
45. **Veis, D. J., C. M. Sorensen, J. R. Shutter, and S. K. Korsmeyer.** 1993. Bcl-2-deficient mice demonstrate fulminant lymphoid apoptosis, polycystic kidneys, and hypopigmented hair. Cell **75:**229–240.
46. **Wang, S., and T. Hazelrigg.** 1994. Implications for bcd mRNA localization from spatial distribution of exu protein in *Drosophila* oogenesis. Nature **369:**400–403.
47. **Ward, W. W.** 1981. *In* M. A. DeLuca and W. D. McElroy (ed.), Bioluminescence and chemiluminescence, p. 235–242. Academic Press, New York, N.Y.
48. **Wolf, K., S. F. Snieszko, C. E. Dunbar, and E. Pyle.** 1960. Virus nature of infectious pancreatic necrosis in trout. Proc. Soc. Exp. Biol. Med. **104:**105–108.
49. **Wu, J. L., H. M. Lin, F. J. Tang, G. G. H. Kou, and K. C. Liu.** 1983. Isolation and characterization of IPNV from rainbow trout in Taiwan, p. 59–67. *In* Proceedings of the Republic of China and Japan Cooperative Science Seminar on Fish Diseases.
50. **Wu, J. L., C. Y. Chang, and Y. L. Hsu.** 1987. Characteristics of an infectious pancreatic necrosis-like virus isolated from Japanese eel (*Anguilla japonica*). Bull. Inst. Zool. Acad. Sin. **26:**201–214.
51. **Wyllie, A. H., J. F. R. Kerr, and A. R. Currie.** 1980. Cell death: the significance of apoptosis. Int. Rev. Cytol. **68:**251–306.
52. **Wyllie, A. H., R. G. Morris, A. L. Smith, and D. Dunlop.** 1984. Chromatin cleavage in apoptosis: association with condensed chromatin morphology and dependence on macromolecular synthesis. J. Pathol. **142:**67–77.